Title

Wnt4 from the Niche Controls the Mechano-Properties and Quiescent State of Muscle Stem Cells

Journal

Cell Stem Cell, 25(5)

ISSN

1934-5909

Authors

Eliazer, Susan
Muncie, Jonathon M
Christensen, Josef
et al.

Publication Date

2019-11-01

DOI

10.1016/j.stem.2019.08.007

Peer reviewed

HHS Public Access

Author manuscript

Cell Stem Cell. Author manuscript; available in PMC 2020 November 07.

Published in final edited form as:

Cell Stem Cell. 2019 November 07; 25(5): 654–665.e4. doi:10.1016/j.stem.2019.08.007.

Wnt4 from the niche controls the mechano-properties and quiescent state of muscle stem cells

Susan Eliazer[1], **Jonathon M. Muncie**[2,4], **Josef Christensen**[3], **Xuefeng Sun**[1], **Rebecca S. D'Urso**[1], **Valerie M. Weaver**[4,5], **Andrew S. Brack**[1,*]

[1]The Eli and Edythe Broad Center for Regenerative Medicine and Stem Cell Research, Department of Orthopaedic Surgery, University of California San Francisco, San Francisco, California 94143, USA.

[2]Graduate Program in Bioengineering, University of California San Francisco and University of California Berkeley, San Francisco, California 94143, USA.

[3]Center of Regenerative Medicine, Massachusetts General Hospital, 185 Cambridge Street, Boston, MA 02114, USA.

[4]Center for Bioengineering and Tissue Regeneration, Department of Surgery, University of California San Francisco, San Francisco, California 94143, USA.

[5]Department of Anatomy, Department of Bioengineering and Therapeutic Sciences, Eli and Edythe Broad Center of Regeneration Medicine and Stem Cell Research and Helen Diller Comprehensive Cancer Center, University of California San Francisco, San Francisco, CA 94143, USA.

SUMMARY

Satellite cells (SCs) reside in a dormant state during tissue homeostasis. The specific paracrine agents and niche cells that maintain SC quiescence remain unknown. We find that Wnt4 produced by the muscle fiber, maintains SC quiescence through RhoA. Using cell specific inducible genetics, we find that a Wnt4-Rho signaling axis constrains SC numbers and activation during tissue homeostasis in adult mice. Wnt4 activates Rho in quiescent SCs to maintain mechanical strain, restrict movement in the niche and repress YAP. The induction of YAP upon disruption of RhoA, is essential for SC activation under homeostasis. In the context of injury, the loss of Wnt4 from the niche accelerates SC activation and muscle repair, whereas overexpression of Wnt4 transitions SCs into a deeper state of quiescence and delays muscle repair. In conclusion, the SC

*Lead Contact; Correspondence to andrew.brack@ucsf.edu.

AUTHOR CONTRIBUTIONS. SE designed and performed experiments, analyzed data, interpreted results and wrote the manuscript. JMM performed experiments, analyzed data and edited the manuscript. JC performed experiments and analyzed data. XS performed experiments and analyzed data. RSD performed experiments. VMW edited the manuscript. ASB conceived the project, designed and interpreted experiments, and wrote the manuscript.

DECLARATION OF INTERESTS.

The authors declare no competing interests.

pool undergoes dynamic transitions during early activation with changes in mechano-properties and cytoskeleton signaling preceding cell cycle entry.

Graphical Abstract

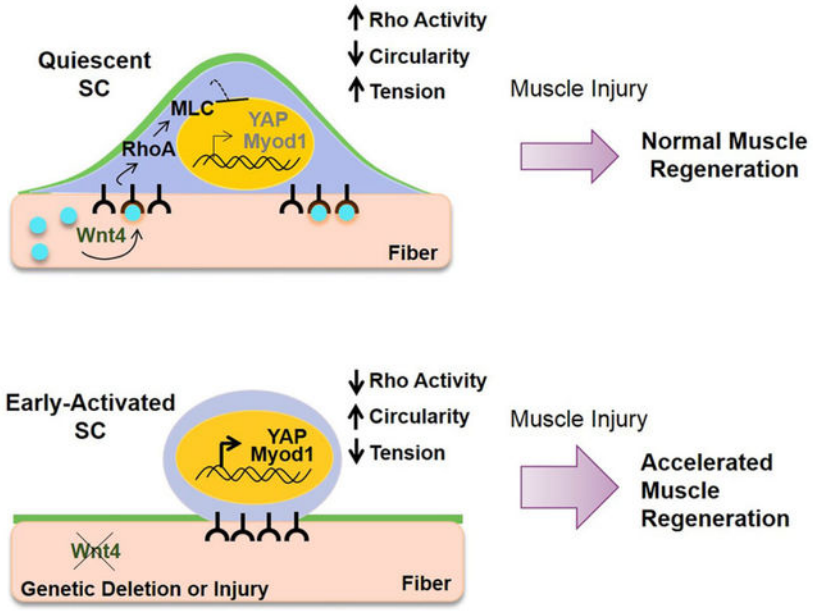

INTRODUCTION

Muscle Stem Cells or Satellite Cells (SCs), are essential for the regenerative capacity of skeletal muscle. SCs reside in a quiescent and immotile state wedged between the basal lamina and the sarcolemma of the muscle fiber (the niche) (Bischoff, 1990). In response to injury, SCs exit this dormant state and transition towards activation, which includes metabolic activation, cell cycle entry and migration. Once dividing, the majority of SCs differentiate, while a subset self-renew to restore the quiescent SC pool.

The quiescent state is critical to maintain stem cell capacity across different niches (Cheung and Rando, 2013; Orford and Scadden, 2008). In contexts of increased SC turnover such as in muscular dystrophy, aging, or in transgenic mice harboring cell cycle mutations, SC function is impaired (Brack and Munoz-Canoves, 2016; Brack and Rando, 2007; Chakkalakal et al., 2014) For many years, SC quiescence has been considered to be a reversible but homogenous state, denoted by the absence of proliferation, and regulated by cell intrinsic regulators (Bjornson et al., 2012; Boonsanay et al., 2016; Cheung et al., 2012; Mourikis et al., 2011). A quiescent intermediate state referred to as G_{Alert} was characterized (Rodgers et al., 2014). This transition state is metabolically active, dependent on mTORC1 and can be induced by systemic HGFA (Rodgers et al., 2014; Rodgers et al., 2017). SCs in G_{Alert}, enter the cell cycle more rapidly, and mount a more efficient regeneration process, and retain stem cell capacity. The mechanisms that promote or repress the transition from quiescence to activation are not well understood.

The niche is a conserved regulator of stem cell quiescence and maintenance. A fundamental but unanswered question in stem cell biology is the identity of specific cell types and paracrine-acting factors that control quiescence and the transition towards activation. The Wnt signaling pathway has been demonstrated to act as a conserved regulator of stem cell function via canonical (β-catenin) and non-canonical (Planar Cell Polarity (PCP) and calcium) signaling (Clevers et al., 2014). However, there is a dearth of information addressing the requirement of specific Wnt ligands, in part due to the possible redundancy between the 19 family members. Recent studies have disrupted Wnt activity using Porcupine (*Porcn*) or *Wntless* loss of function alleles in different tissues to disrupt the processing of the Wnt ligand family (Nabhan et al., 2018; Tammela et al., 2017; Zepp et al., 2017). While these studies provide proof of principle for the importance of Wnt ligands, they did not elucidate the identity of the Wnt family members. Wnt signaling plays a critical role in coordinating SC state transitions from asymmetric fate, proliferation, commitment and differentiation (Brack et al., 2008; Brack et al., 2009; Jones et al., 2015; Lacour et al., 2017b; Le Grand et al., 2009; Parisi et al., 2015b; Rudolf et al., 2016). Whether Wnt ligands, from an anatomically defined niche cell, controls SC quiescence remains unknown. Identifying the niche and signaling molecules that regulate quiescence is critical to understanding regenerative biology and the development of therapeutics to harness stem cell function.

Using an inducible genetic approach to specifically target the SC niche, we provide the first evidence of a paracrine-acting niche factor, Wnt4, that reinforces SC quiescence through activation of Rho-GTPase and repression of YAP (Yes-Associated Protein). In conclusion, Wnt4 levels dictate the depth of SC quiescence during homeostasis, their activation response and regenerative potential.

RESULTS.

Wnt4 from the muscle fiber maintains adult SC quiescence.

To identify Wnts that regulate SC quiescence in the adult muscle, we first analyzed Wnt ligand expression by microarray analysis and qRT-PCR, on freshly isolated single muscle fibers. Although a number of different Wnts were expressed, Wnt4 was significantly enriched in uninjured muscle fibers (Figure 1A, 1B). We next assessed Wnt4 transcript levels in whole muscle during the early stages of muscle repair (Polesskaya et al., 2003). We find that Wnt4 transcript levels are between 45–65% lower at 18, 24 and 48 hours after $BaCl_2$ injury, compared to muscles of non-injured mice (Figure 1C, S1A). Receptivity of the quiescent SCs (QSCs) to Wnt ligand was indicated by the expression of most Frizzled receptors in freshly isolated FAC-sorted SCs (Figure S1B). It should be noted that the isolation of SCs by FACS (3 hours) or single muscle fibers (90 minutes) will induce some activation (Machado et al., 2017; van den Brink et al., 2017; van Velthoven et al., 2017). For the purpose of this study we will refer to the freshly isolated SCs as QSCs.

To test the requirement of niche-derived Wnt4 for SC quiescence *in vivo*, we conditionally deleted Wnt4 (Kobayashi et al., 2011) in adult muscle fibers, using tamoxifen (tmx)-inducible Crerecombinase under the control of Human Skeletal Actin (McCarthy et al., 2012) (Tg: $HSA^{CreMER/+}$; $Wnt4^{fl/fl}$ herein called as Myofiber (MF)-$Wnt4^{fl/fl}$). This

transgenic line provided stringent and efficient recombination in adult muscle fibers (Figure S1C, S1D). Adult mice (3–4 months old) were given tmx for 5 days followed by a 6-day or 14-day chase (Figure 1D). BrdU was given in the drinking water during the chase to label cycling SCs. We observed an increase in the number of SCs (Figure 1E, 1F), the fraction that incorporated BrdU (Figure 1G), and expressed MyoD in a Wnt4-depleted niche compared to controls (Figure 1H, 1J). To confirm that niche-derived Wnt4 regulated SC quiescence, we stained muscle sections with DDX6, a marker of mRNP granules, that is lost when SCs break quiescence (Crist et al., 2012; Goel et al., 2017). We found that DDX6 levels decreased in SCs from a Wnt4-depleted niche compared to controls (Figure 1I, 1K). Loss of SC quiescence is often associated with precocious differentiation and fusion into existing muscle fibers (Bjornson et al., 2012; Mourikis et al., 2012). In spite of the ~2-fold expansion of the SC pool, we found no evidence of central-located nuclei in the myofibers or $BrdU^{+}$/$Pax7^{-}$ nuclei underneath the basal lamina.

Porcupine (Porcn) is essential for Wnt ligand processing and secretion (Kadowaki et al., 1996; Proffitt and Virshup, 2012). Therefore we used a conditional gene deletion approach (Roman et al., 2014) to disrupt Porcn function and hence Wnt paracrine action, in adult muscle fibers (Figure S1E). We find a similar increase in the number of SCs in a Porcn-depleted niche relative to controls, as observed for Wnt4 depletion (Figure S1F). *In vitro*, SCs activated more rapidly in a Porcn-depleted niche, which was abrogated by treatment with recombinant Wnt4 (Figure S1G), suggesting that Wnt4 plays a dominant role in maintaining SC quiescence. Together, these results demonstrate that Wnt activity from muscle fibers is required for SC quiescence through paracrine action.

Wnt4 is known to play a role in vertebrate neuromuscular junction (NMJ) formation (Strochlic et al., 2012). Loss of NMJ activity results in muscle fiber atrophy and a well-defined ‘denervation’ transcriptional response (Hyatt et al., 2003; Windisch et al., 1998). We find no differences in muscle fiber size in muscle sections (Figure S1H), denervation transcript response (Figure S1I–S1K) or myosin expression (Figure S1L) from single muscle fibers at homeostasis. These data suggest that Wnt4 depletion does not induce atrophy or denervation in adult muscle fibers, suggesting Wnt4 plays a different role on the NMJ between development and adult homeostasis. In conclusion, Wnt4 from the niche is critical for maintaining SC quiescence during tissue homeostasis.

Niche-derived Wnt4 regulates muscle regenerative potential.

In response to an injury stimulus, quiescent SCs enter the cell cycle. We asked whether depletion of Wnt4 from the niche influenced cell cycle entry. Upon mitogen stimulation *in vitro*, compared to controls, the majority of SCs on single muscle fibers from a Wnt4-depleted niche and Porcn-depleted niche rapidly activated ($MyoD^{+}$) and entered the cell cycle as measured by EdU (Figure 2B, S2A–S2C).

We next tested the effect of niche-derived Wnt4 on the ability of SCs to regenerate muscle. In the tmx-inducible $HSA^{CreMER/+}$.$Wnt4^{fl/fl}$ genetic model, adult fibers are depleted of Wnt4, but the SCs are wildtype. In response to injury, wildtype SCs formed wildtype muscle (Figure S2D, S2E). Therefore, any regenerative phenotype observed after Wnt4 deletion is directly due to the altered niche signal prior to injury. We found that the size of regenerating

muscle fibers (6 days after injury) was significantly increased and the percentage of eMHC^{+} fibers decreased, after Wnt4 depletion in the niche compared to control mice (Figure 2C–2E). The number of proliferating Pax7^{+} SCs increased after 6 days of regeneration in Myofiber-Wnt4$^{fl/fl}$ compared to controls (Figure S2F, S2G). No difference in fiber size was observed between the control and Wnt4-depleted niche 35 days after injury (Figure S2H). However, compared to controls, the number of SCs remains elevated in Myofiber-Wnt4$^{fl/fl}$ (Figure S2I). Therefore, the SC pool and fiber size was restored to pre-injury levels.

To determine if increasing Wnt4 in the niche reinforces quiescence, we used an inducible transgenic gain-of-function approach to overexpress Wnt4 (Lee and Behringer, 2007) in adult muscle fibers (Tg: HSA$^{CreMER/+}$; Wnt4$^{OX/+}$ herein called as Myofiber (MF)-Wnt4$^{OX/+}$) (Fig. 2F, S2J). In cross sections of uninjured muscle, DDX6 expression was increased in Myofiber-Wnt4$^{OX/+}$ compared with controls (Figure 2G, 2H). Upon mitogen stimulation *in vitro*, compared to controls, the majority of SCs from a Wnt4-overexpressed niche remained in a quiescent (MyoD^{-}) state (Figure 2I). In response to injury, muscle fiber size was smaller and the percentage of eMHC fibers greater in Myofiber-Wnt4^{OX}, compared to controls (Figure 2J–2L). These data suggest that Wnt4 from the niche is sufficient to reinforce SC quiescence and delay muscle regeneration. Therefore, the levels of a single Wnt ligand (Wnt4) from a single type of niche cell (the muscle fiber) regulates the depth of SC quiescence and muscle regenerative potential.

Niche-derived Wnt4 stimulates RhoA activity and cytoskeletal signaling.

Wnt ligands signal in a paracrine manner through canonical or non-canonical pathways (Komiya and Habas, 2008). To identify the signaling mechanism transducing Wnt4 signals in the ‘receiving’ cell, we analyzed canonical markers, active β-catenin, on single muscle fibers and *Axin2*, in sorted QSCs. The deletion of Wnt4 and Porcn in the niche did not change canonical Wnt signaling in QSCs (Figure 3A–3C and Figure S3A). Therefore, Wnt4 does not signal through canonical Wnt signaling. Moreover, SCs in a Wnt4-depleted niche are not transitioning to a myogenic progenitor state, as defined by the accumulation of β-catenin (Figeac and Zammit, 2015; Goel et al., 2017; Murphy et al., 2014; Parisi et al., 2015a). In addition, analysis of muscle fibers for autocrine canonical β-catenin signaling revealed no change in active β-catenin levels in Myofiber-Wnt4$^{fl/fl}$ muscle fibers when compared to control (Figure S3B, S3C). Therefore, Wnt4 signals via non-canonical Wnt signaling cascade in QSCs.

Rho GTPase is a well-characterized downstream component of non-canonical Wnt signaling pathway, first identified during gastrulation, to promote polarized cell shape changes and migration (Habas et al., 2003; Schlessinger et al., 2009). The Rho family of GTPases play a key role in cytoskeletal remodeling (Sit and Manser, 2011) and has been implicated in HSC self-renewal (Schreck et al., 2017). We found that active Rho was reduced in sorted QSCs from a Wnt4-depleted niche compared to controls (Figure 3D, 3E). We next treated sorted SCs from Myofiber-Porcn$^{fl/fl}$ or controls with vehicle or Wnt4 recombinant protein for 4 hours and assayed for active Rho. We found that compared to control, the levels of active Rho were decreased in vehicle-treated SCs from a Porcn-depleted niche, and was rescued by Wnt4 treatment (Figure S3E).

To investigate the highly interconnected cytoskeletal network in QSCs, we analyzed phosphorylated-Myosin Light Chain (pMLC), a downstream target of Rho that regulates acto-myosin assembly, contraction and stress fiber formation (Chrzanowska-Wodnicka and Burridge, 1996; Kimura et al., 1996). pMLC was expressed at lower levels in SCs on isolated single muscle fibers from a Wnt4-depleted niche than the controls (Figure 3F, 3G). Rho regulates the formation of stress fibers and focal adhesions (Ridley and Hall, 1992). Phosphorylated-Focal Adhesion Kinase (pFAK), a regulator of focal adhesions was also decreased in SCs in a Wnt4-depleted and Porcn-depleted niche (Figure 3H, 3I and S3D). Consistent with a paracrine effect from Wnt4 on QSCs, cytoskeletal signaling components were not differentially expressed on single muscle fibers from Myofiber-Wnt4$^{fl/fl}$ and controls (Figure S3F–S3I). Therefore, Wnt4 from the niche stimulates Rho activity and cytoskeletal signaling in QSCs.

Wnt4 regulates mechano-properties and niche retention in QSCs.

Cells rapidly respond to mechanical cues from the cytoskeleton by changing their cell shape, tension and migration (Burridge and Guilluy, 2016). We observed that SCs resident on isolated single muscle fibers in a Wnt4-depleted niche have a more rounded shape than the controls (Figure 4A). We used Atomic Force Microscopy (AFM) to measure tension of sorted QSCs. We found that stiffness of QSCs was ~50% less from a Wnt4-depleted niche compared to controls, and similar to the stiffness of QSCs treated with a Rho inhibitor (Figure 4B). We observed that 33% of SCs in a Wnt4-depleted niche were located in the interstitial space, outside the basal lamina *in vivo* (Figure 4C, 4D). Using a tmx-inducible SC specific approach to reduce Rho *in vivo* (Jackson et al., 2011) (Tg: Pax7$^{CreER/+}$; RhoA$^{fl/+}$ herein called SC-RhoA$^{fl/+}$), we found 35% of SCs were located outside the niche after a reduction in Rho (Figure 4E, 4F). All these results taken together, demonstrate that a signaling axis, initiated by Wnt4 and transmitted by Rho, regulates stiffness and niche-retention of QSCs.

To catalogue the temporal changes in cytoskeletal signaling, mechano-properties and cell cycle entry, we performed a detailed time-course during the transition between SC quiescence and activation on single muscle fibers *in vitro*, using markers of morphometric adaption (cell size and shape), cytoskeletal signaling (pMLC), mechano-transduction (YAP), mTORC1 activation (pS6) and cell cycle entry (MyoD). During the first few hours of mitogen exposure there was an increase in circularity and decrease in size, coincident with the decline in pMLC levels. Contrasting the decline in pMLC, was the upregulation of pS6, which was followed by an increase in cell size and induction of MyoD and YAP (Figure 4G–4I and S4A–S4F). If these data are viewed as time representing the stages to activation, then cell shape (circularity) and cytoskeletal changes (pMLC) precede cell cycle entry (MyoD) and mechanotransduction (YAP), but are broadly coincident with entry into a G_{alert}-like state (pS6+) (Rodgers et al., 2014). Therefore, changes in cytoskeletal signaling and mechano-properties are early events during the transition between quiescence and activation.

Wnt4-Rho signaling axis maintains SC quiescence

The dynamics of SC morphology and cytoskeletal signaling during SC activation and in response to Wnt4 depletion from the niche, prompted us to ask whether the decrease in Rho

and cytoskeletal signaling was sufficient to induce SC activation in uninjured muscle. To answer this question, we analyzed SC-RhoA$^{fl/+}$ and littermate control mice. We found lower levels of active Rho (sorted SCs) and pMLC (SCs on single muscle fibers) (Figure 5A, 5B), an expanded SC pool (Figure 5C) and increased BrdU+/Pax7+ SCs (Figure 5D) (in muscle sections) in SC-RhoA$^{fl/+}$ mice compared to controls. Consistent with the expansion of SCs in uninjured muscle; through the reduction in Rho (in QSCs) or Wnt4 (from the niche), acute treatment of isolated wildtype single muscle fibers with a Rho inhibitor, accelerated cell cycle entry of SCs, as measured by MyoD expression and EdU incorporation (Figure 5E and Figure S5A). Therefore, Rho acts in a cell-autonomous manner to maintain SC quiescence under tissue homeostasis, and repress cell cycle entry in response to mitogen stimulation.

Rho GTPase activates Rho kinase (ROCK), which either directly activates MLC or inactivates myosin phosphatase, subsequently activating MLC (Kimura K et al, 1996). We found that SCs on isolated wildtype single muscle fibers activated more rapidly *in vitro* in the presence of ROCK inhibitor (Figure 5E), suggesting that SC quiescence is regulated through a Rho-ROCK axis. Finally, we asked whether active Rho could repress activation of SCs in a Wnt4-depleted niche. In control single muscle fibers, transient Rho activation maintained the quiescent state, whereas in a Wnt4-depleted niche, Rho activation reestablished quiescence in a dose-dependent manner (Figure 5F, S5B). Moreover, adding active Rho to SCs on a Wnt4-depleted niche restored pMLC and pS6 levels to those observed in control SCs (Figure 5G, S5C). Together these results demonstrate that Wnt4 from the niche stimulates Rho activity to reinforce SC quiescence.

The temporal coincidence of pS6 (mTORC1 signaling) induction and pMLC (cytoskeletal signaling) decline during the transition from quiescence to activation (Figure 4H, S4C, S4D), and the rapid cell cycle entry in response to mitogen from Wnt4- and Porcn-mutant niches (Figure S2B, S2C), is reminiscent of the mTORC1-driven, G_{Alert} state (Rodgers et al., 2014). Therefore, we asked whether Wnt4 represses mTORC1 activity to reinforce SC quiescence during tissue homeostasis. First, we used pS6 as a marker of mTORC1 activity, and thus the G_{Alert} state. Similar to previous results, 35% of SCs were pS6^{+} in control single muscle fibers, suggesting that a fraction of QSCs are in a G_{Alert}-like state under homeostasis. In a Wnt4 and Porcn-depleted niche, the percentage of pS6^{+} QSCs increased to 50% (Figure 5H, 5I, S5D). Therefore, Wnt4 acts as a repressor of a G_{Alert}-like state. To query whether the increased mTORC1 signaling in a Wnt4-depleted niche was required for SC activation during tissue homeostasis, we treated mice with a Wnt4-depleted niche and controls with Rapamycin continuously and analyzed the SCs 14 days after tamoxifen (Figure S5E). Rapamycin treatment decreased pS6 (Figure S5F) and pFAK levels (Figure S5G) on single muscle fibers. However, SC number, pMLC expression and cell shape were not rescued (Figure S5H–S5J). Moreover, pS6 activity and pFAK levels were not altered in SCs from SC-RhoA$^{fl/+}$ compared to control mice (Figure 5J, S5K). Since pFAK levels are responsive to Rapamycin, pFAK could be downstream of mTORC1 signaling. In conclusion, these data demonstrate that Wnt4-Rho signaling regulates SC quiescence during tissue homeostasis, independent of mTORC1 activity. Contrary to the *in vivo* Rho mutant data, where the reduction in Rho had no effect on pS6 and pFAK activity, the treatment of freshly-isolated wildtype muscle fibers with Rho inhibitor caused a rapid upregulation of pS6 and a

decline in pFAK levels (Figure S5L, S5M). These results suggest that in the presence of growth factors or nutrients, Rho engages mTORC1 and FAK as SCs transition towards activation.

YAP is a downstream effector of Wnt4-Rho signaling

YAP has been implicated in mechano-transduction (Dupont et al., 2011) and is required for SC activation (Judson et al., 2012; Sun et al., 2017). We reasoned that YAP could be involved in the loss of SC quiescence in contexts of reduced Wnt4-Rho signaling. Therefore, we analyzed Wnt4 (niche) and Rho (SC) mutant mice for YAP expression. We found *YAP* transcript was elevated in sorted SCs from Myofiber-Wnt4$^{fl/fl}$ mice compared to the controls (Figure 6A). Consistent with previous reports, YAP protein was not expressed in QSCs in controls (Judson et al., 2012). In contrast, we found increased nuclear YAP protein expression in SCs on isolated muscle fibers from Myofiber-Wnt4$^{fl/fl}$ and SC-Rho$^{fl/+}$at 6 and 14 days post-tmx (Figure 6B–6D). We did not detect cytoplasmic YAP (Judson et al., 2012). Therefore, a Wnt4-Rho signaling axis repressed YAP in QSCs. To ask whether YAP was required for the loss of quiescence in response to disrupted Wnt4-Rho signaling, we deleted YAP (Xin et al., 2011) in a SC-RhoA$^{fl/+}$ background (Tg: Pax7$^{CreER/+}$; RhoA$^{fl/+}$; YAP$^{fl/fl}$ herein called as SC-RhoA$^{fl/+}$-YAP$^{fl/fl}$) and analyzed the SC response 14 days post-tmx (Figure 6E). Quantification on muscle sections revealed that deletion of YAP prevented SC expansion (Figure 6F), activation (Figure 6G) and proliferation (Figure 6H) when Rho was reduced. Therefore, Rho activity maintained SCs in a quiescent state through repression of YAP (Figure 6I).

DISCUSSION

Despite the numerous studies on the role of Wnt signaling in adult stem cell biology, there is little known about the specific Wnt ligands, their source and how they signal to stem cells *in vivo* (Clevers et al., 2014). Our results provide direct evidence of a specific paracrine-acting Wnt from a defined niche cell that is required to maintain mammalian stem cell quiescence during tissue homeostasis. We find that Wnt4 is produced in adult muscle fibers, activates Rho-GTPase and represses YAP within the SCs, to maintain quiescence during tissue homeostasis. In the absence of niche-derived Wnt4, SCs transition towards a more activated state which accelerates muscle tissue repair in adult mice.

The Wnt signaling pathway is divided into two branches; a canonical and non-canonical arm, based on the involvement of β-catenin (Komiya and Habas, 2008). While the specific Wnt ligands required for canonical signaling during SC lineage progression remain unknown, it is clear that SC proliferation and differentiation depend on intracellular canonical Wnt signaling. Whereas, asymmetric division of activated SCs and myotube hypertrophy depend on non-canonical Wnt signaling (Lacour et al., 2017a; Le Grand et al., 2009; von Maltzahn et al., 2012). Therefore, Wnt signaling plays critical roles during SC lineage progression. In quiescent SCs, we find undetectable levels of nuclear β-catenin and low levels of Axin2. Therefore, we propose that canonical Wnt signaling is inactive in QSCs. Rather, non-canonical Wnt signaling is active and functionally required for SC quiescence. Wnt ligands can act antagonistically (Mikels and Nusse, 2006; Topol et al.,

2003; Westfall et al., 2003), leading to either intracellular canonical or non-canonical Wnt signaling. In the present study, deletion of Wnt4 and Porcn from adult fibers did not induce canonical signaling, arguing against antagonism between canonical and non-canonical Wnt signaling in QSCs. With the generation of inducible genetic approaches, it is now possible to define the cell sources and specific Wnt ligands required for SC function during tissue homeostasis and regeneration.

The Wnt-PCP pathway has been widely studied in Drosophila, Xenopus and Zebrafish. Specific Wnt family members including Wnt5, Wnt11 and Wnt4 signal via Frizzled receptors to Dishevelled (Dvl), an adaptor protein which becomes polarized at the apical membrane to regulate morphology, polarization and migration of cell structures in the developing epithelium (Jussila and Ciruna, 2017; Sokol, 2015; Yang and Mlodzik, 2015). The defining feature of this pathway is its regulation of the actin cytoskeleton via Rho-GTPase (Schlessinger et al., 2009). Therefore, we define a requirement for Wnt-PCP signaling in adult mammalian muscle stem cell quiescence.

Our data provide evidence that Wnt4-Rho signaling represses YAP activity in QSCs *in vivo*. We find that YAP induction is required for SCs to break quiescence under homeostatic conditions. YAP is a sensor and transducer of mechanical stimuli, that functions downstream of Hippo signaling or independently through the actin cytoskeleton. The latter is consistent with the present data showing a role for Rho in the repression of YAP. In the context of reduced Rho, YAP inhibition prevented SC expansion, consistent with the requirement for YAP in SC proliferation (Judson et al., 2012). However, previous work demonstrated that induction of a stabilized form of YAP was not sufficient to induce SC proliferation (Tremblay et al., 2014). At present we cannot exclude that differences in the methods used to analyze SC number and activation state, or the level of YAP between the two experimental contexts, might explain these discrepancies. We suggest that a reduction in cytoskeletal signaling in QSCs lowers their threshold for activation by decreasing cellular stiffness.

While the polarity protein, Dvl is sufficient and required for PCP signaling, its role has not been examined in SCs. It will be interesting to examine whether Wnt4 regulates polarity proteins and whether they interact with Dvl in quiescent SCs. For example, Mpp7, a component of Hippo signaling, is expressed in QSCs to inhibit YAP activity and thus limit SC activation (Li and Fan, 2017). In QSCs, we and others, did not detect YAP protein in the cytoplasm or at the plasma membrane. Upon SC activation, YAP expression increases in the nucleus (Judson et al., 2012). We find that nuclear YAP can be detected within a few hours of activation stimuli. This suggests a transcriptional component to YAP induction during early stages of SC activation.

In vitro studies have examined YAP activation and its nuclear localization after altering cellular and extracellular mechanics by altering F-actin accumulation using inhibitors or plating cells on a soft or stiff matrix (Dupont, 2016; Seo and Kim, 2018). Increased formation of actin stress fibers and contractility leads to activation of YAP (Seo and Kim, 2018). *In vivo* we see an opposite effect: decreasing stiffness of QSCs through a reduction of Wnt4 from the niche or reducing Rho levels in SCs, causes an activation and nuclear localization of YAP. This suggests a context-dependent role of cytoskeletal stiffness and

YAP activity. Further investigation is needed to understand if actin signaling directly represses YAP activity in QSCs *in vivo*.

Analysis of whole muscle revealed that Wnt4 transcript levels decreased during early stages of regeneration after $BaCl_2$ injury (Figure 1C, S1A). It has been reported that Wnt4 levels undergo a transient increase before decreasing, in response to cardiotoxin injury (Polesskaya et al., 2003). It is possible that the type of injury, in this case $BaCl_2$ versus cardiotoxin, elicits a different cellular response (Morel et al., 2009). Studying paracrine regulation between different cell types within regenerating muscle tissue could uncover new modes of intercellular communication.

The important role of mechano-properties on cell fate across different contexts from development to stem/progenitor differentiation *in vitro* is becoming appreciated (Behrndt et al., 2012; Engler et al., 2006; Gilbert et al., 2010). The decision of activated SCs to self-renew or differentiate can be skewed based on the stiffness of the ECM. We find that disruption of Wnt4-Rho signaling decreases the stiffness and displacement of SCs from the niche. Therefore, a specific niche factor, acting in a paracrine manner alters the mechanical properties and quiescent state of an adult mammalian stem cell.

Consistent with the notion that quiescence is essential for adult stem cell preservation, deregulation of quiescence in muscle stem cells during tissue homeostasis, leads to their depletion through apoptosis, precocious differentiation or incorporation into the center of the muscle fiber-reminiscent of a regenerative event (Bjornson et al., 2012; Cheung et al., 2012; Goel et al., 2017; Mourikis et al., 2012). In contrast, the results in the present study and those of Goel et al (Goel et al., 2017), suggest that the SC pool can establish a new homeostatic setpoint. While there are many possibilities that explain the discrepancy, including the cell type and specific genes that are disrupted; based on the present results SC depletion, differentiation and fusion are not obligate when quiescence is broken during tissue homeostasis.

Preservation of the SC pool after injury is critical for long-term tissue homeostasis. In response to injury, we observed an expanded SC pool, in the Wnt4 mutant compared to control muscle. Interestingly, pool size was restored to pre-injured levels. We would have predicted that after Wnt4 deletion from the niche, the SC pool would return back to control levels, due to the reformation of muscle fibers and the SC pool by genetically wildtype (non-recombined) SCs. Rather our data raises a couple of intriguing possibilities: 1) Wnt4 in regenerating myofibers does not set the size of the SC post-injury, 2) the size of the SC pool in regenerated muscle is instructed prior to injury, i.e. in the QSCs, to regulate a return to the homeostatic setpoint. If true, this would involve a counting mechanism at the level of the stem cell or available niche sites, or 3) Wnt4 from the niche regulates the number of asymmetric and symmetrically dividing daughters. This is less likely due based on the decline in Wnt4 levels upon injury. These possibilities warrant further investigation.

To fulfill their roles during tissue repair, stem cells must exit quiescence, proliferate and mobilize to the site of injury. During the transition between quiescence and activation, SCs pass through a distinct molecular and functional state termed G_{alert}, denoted by its increase

in cell size and mTORC1 activation (Rodgers et al., 2014). Acute induction of the G_{alert} state promotes muscle repair (Rodgers et al., 2014; Rodgers et al., 2017). In the present study we used single cell analysis to dissect novel molecular states as SCs break quiescence. Our data reveal that the quiescent SC pool undergoes dynamic transitions, with changes in morphology, mechano-properties and cytoskeleton signaling preceding cell cycle entry. Using time-lapse imaging we recently demonstrated that SC motility occurs early in the activation response (Kimmel et al., 2018). Based on the timepoints we analyzed *in vitro* in the present study, changes in cytoskeletal signaling either precede or are coincident with mTORC1 activation, followed by induction of YAP and MyoD. We speculate that a decrease in Wnt4-Rho signaling initiates a migration program to reach an injury site, coupled with the energy and biomass, which licenses QSCs for activation. In line with the concept that the cytoskeletal machinery functions as an early regulator of SC activation, mir-708, upregulates Tensin3, a positive regulator of pFAK activity, to delay cell cycle entry (Baghdadi et al., 2018). In the present study, we find that inhibition of Rho decreased mTORC1 and pFAK *in vitro*. Whereas RhoA deletion in SCs in uninjured muscle *in vivo* did not affect mTORCl and pFAK. Therefore, it is possible that pFAK, which is regulated by mTORC1 activity *in vitro* (Figure S5G) is part of a molecular pathway deployed when SCs break quiescence in a stimulatory (mitogenic or injured) environment. This would suggest a rapid remodeling of the signaling pathways regulated by Rho in the absence or presence of activation stimuli. This awaits further investigation.

Using inducible cell specific genetic approaches to target a component of the muscle stem cell niche-the muscle fiber, we demonstrate that Wnt4 regulates the depth of SC quiescence under tissue homeostasis, and regenerative potential in response to injury. Our findings have implications for regenerative medicine, as a means to mobilize quiescent stem cells and facilitate tissue repair after injury or in disease.

STAR METHODS

LEAD CONTACT AND MATERIALS AVAILABILITY

Further information and requests for resources and reagents should be directed to and will be fulfilled by the Lead Contact, Andrew S. Brack (andrew.brack@ucsf.edu).

EXPERIMENTAL MODEL AND SUBJECT DETAILS

Animals—Mice were housed and maintained in accordance with the guidelines of the Laboratory Animal Research Center (LARC) of University of California, San Francisco. Previously published HSA^{CreMER} (McCarthy et al., 2012), $Wnt4^{flox/flox}$ (Kobayashi et al., 2011), $Wnt4^{OX/+}$ (Lee and Behringer, 2007), $Porcn^{flox/flox}$ (Roman et al., 2014), $Pax7^{CreER}$ (Nishijo et al., 2009), $RhoA^{flox/+}$ (Jackson et al., 2011), $YAP^{flox/flox}$ (Xin et al., 2011) were used in this study. $Rosa26^{mTmG}$ and C57BL/6 were obtained from Jackson Laboratory. All mice used for experiments were adults, between 12–16 weeks of age. The control and experimental mice used are littermates in all experiments. Approximately equal numbers of male and female mice were used in all experiments. Animals were genotyped by PCR using tail DNA. Primer sequences are available upon request.

METHOD DETAILS

Animal Procedures—Tamoxifen (Sigma) was dissolved in corn oil at a concentration of 20mg/ml. Both control and experimental mice were administered tamoxifen at a concentration of 150mg/kg per day for five continuous days (for HSA^{CreMER} mice) or 7 continuous days (for $Pax7^{CreER}$ mice) by intraperitoneal injection. To assess *in vivo* cell proliferation, control and experimental mice were administered 0.5mg/ml Bromodeoxyuridine (BrdU) (Sigma) in drinking water supplemented with 5% sucrose continuously throughout the course of the experiment starting from the 3rd day of tamoxifen. Rapamycin (LC Laboratories) was dissolved in 10% Polyethylene glycol 400 (Hampton Research) and 10% Tween 80 (Sigma) and administered intraperitoneally at a dose of 4mg/kg daily starting from the 3rd day of tamoxifen till the end of the experiment (2 weeks of chase) for a total of 17 days.

Muscle Injury—Control and experimental mice were anesthetized by isofluorane inhalation and 50μl of 1.2% $BaCl_2$ was injected into and along the length of the tibialis anterior (TA) muscle. After 6 days or 35 days of regeneration, mice were euthanized and the injured TA muscle was fixed immediately in 4% PFA and frozen in 20% sucrose/OCT medium. 8μm cross-sections of the muscle were made and stained for anti-laminin. 10x images were collected at three regions in the mid-belly of each muscle. Only mice that had more than 80% injury in their TA were analyzed. All the regenerating fibers in the entire TA section were analyzed for fiber size. The average cross-sectional area of the fibers was determined using imageJ software. To assess *in vivo* proliferation during 5.5 to 6 days of muscle regeneration, 10mg BrdU was given to the mice by intraperitoneal injection 12 hours before the mice were sacrificed on day 6.

Sciatic Nerve Transection (Denervation)—C57BL/6 mice were anesthetized by intraperitoneal injections of ketamine at a dose of 100mg/kg and Xylazine at 10mg/kg. The left hindlimb was carefully shaven and a 1mm incision was made in the skin, posterior and parallel to the femur. A small cut is made in the biceps femoris muscle to expose the sciatic nerve. 1–2 mm of the sciatic nerve is cut and the muscle is then closed by stitching. The mice were given an analgesic, buprenorphine at a dose of 0.5mg/kg and allowed to recover on a heated pad. Three days after the surgery, single muscle fibers were isolated from the EDL muscle of the denervated left leg of the mice. Single fibers from the EDL of uninjured mice were used as controls.

Isolation of SCs and Fluorescence Assisted Cell Sorting (FACS)—Satellite cells were isolated from hindlimb and forelimb muscles. The mice were euthanized, the hindlimb and forelimb skeletal muscles were removed, chopped finely and digested using 0.2% Collagenase type 2 (Worthington) in DMEM media for 90 minutes in shaking water bath at 37°C. The digested muscle was washed twice with Rinsing media (Ham's F10, 10% horse serum). A second digestion was performed with 0.2% Collagenase type 2 and 0.4% Dispase (Gibco) in Rinsing media for 30 minutes in shaking water bath at 37°C. The digested tissue was passed through a 20-gauge needle three times, then passed through a 40μm filter and a 20μm filter. The mononuclear muscle cells were stained for PE-Cy7 anti-mouse CD31 (clone 390; BD Biosciences), PE-Cy7 anti-mouse CD45 (clone 30-F11; BD Biosciences),

APC-Cy7 anti-mouse Seal (clone D7; BD Biosciences), PE anti-mouse CD106/VCAM-1 (Invitrogen) and APC anti-α7 integrin (clone R2F2; AbLab). FACS was performed using FACS Aria II (BD Biosciences) by gating for $CD31^{-}/CD45^{-}/Scal^{-}/\alpha7\ integrin^{+}/VCAM1^{+}$ to isolate SCs.

Isolation of Single Muscle Fibers—Single muscle fibers were isolated from the Extensor Digitorum Longus (EDL) muscle of the adult mouse. The EDL muscle was removed from the hindlimb of the mouse and digested with 0.2% Collagenase type I (Gibco) for 90 minutes in shaking water bath at 37°C. Single muscle fibers were obtained by gently triturating the digested muscle using a glass pipet in plating media (DMEM, 10% horse serum). The single fibers were manually collected under a dissection microscope, fixed immediately in 4% PFA for 10 minutes or cultured in plating media.

***In vitro* treatment of single muscle fibers—**The isolated single fibers from the EDL of Control and Myofiber-$Porcn^{fl/fl}$ mice were cultured in plating media (DMEM, 10% horse serum) and treated with either PBS or with recombinant mouse Wnt4 (100ng/ml; R&D systems) for 8 hours. The fibers were then fixed and stained for anti-Pax7 and anti-MyoD. For *in vitro* cell cycle entry assays, single muscle fibers from Control, Myofiber-$Wnt4^{fl/fl}$ and Myofiber-$Porcn^{fl/fl}$ mice were harvested and cultured in plating media containing EdU (10μm; Carbosynth) for 30 hours. Single fibers from C57BL/6 mice were cultured in plating media with either PBS or Rhol inhibitor (0.5 and 1μg/ml; Cytoskeleton Inc.) for different time points: 2h for pS6 and pFAK expression, 8h for MyoD expression and for cell cycle entry, in media containing EdU for 30 hours. Single fibers from C57BL/6 mice were cultured in plating media with either PBS or ROCK inhibitor Y-27632 (3 and 10μM; Stemcell Technologies Inc.) for 8 hours and stained for MyoD protein expression. For *in vitro* rescue experiments, Control and Myofiber-$Wnt4^{fl/fl}$ single muscle fibers were cultured in plating media with PBS or Rho activator (0.5 and lμg/ml; Cytoskeleton Inc.) for different time points: 2h for pMLC and pS6 expression, 8h for MyoD expression and for cell cycle entry, in media containing EdU for 36 hours. The fibers were then fixed and stained for the different antibodies. EdU staining was done using the Click-iT Plus EdU Alexa Fluor™ 594 Imaging Kit (Invitrogen) followed by staining with anti-Pax7 antibody.

Atomic Force Microscopy (AFM)—Cells isolated for AFM were seeded onto chamber slides and placed on the stage of an MFP3D-BIO inverted optical AFM (Asylum Research) mounted on a Nikon TE2000-U inverted microscope. Indentations were made using silicon nitride cantilevers with spring constants ranging from .05 to .07N/m and borosilicate glass spherical tips 5μm in diameter (Novascan Tech). The cantilevers were calibrated using the thermal oscillation method prior to each experiment. Cells were indented at rates ranging from 0.75 to 1.25μm/s with a maximum force of 4.5 nN. The Hertz model was applied to the force curves obtained from each cell indentation to calculate the elastic modulus (Young's modulus, stiffness). Cells were assumed to be incompressible; therefore, a Poisson's ratio of 0.5 was used in the calculation of the elastic modulus.

In situ binding assay for Rho-GTPase activity—FACS isolated SCs were fixed with 4% PFA for 25 minutes. The SCs were then washed with PBS and permeabilized in 0.05%

TritonX100/PBS for 10 minutes. Cells were blocked in 5% FBS/PBS and incubated for an hour at room temperature with GST tagged Rhotekin-Rho binding domain (RBD) (Cytoskeleton Inc.) which binds specifically to active Rho. This is followed by PBS washes and incubation with fluorophore conjugated anti-GST antibody (Invitrogen) and DAPI (Life Technologies) for an hour at room temperature. The cells were washed with PBS and mounted.

Immunostaining—Fixed myofibers were permeabilized with 0.2% TritonX-100/PBS and blocked with 10% goat serum/0.2% TritonX/PBS. Primary antibodies used in this study were: rat anti-BrdU (clone BU1/75; Abcam), mouse anti-Pax7 (DSHB), rabbit anti-MyoD (Santa Cruz Biotechnology) rabbit anti-Laminin (Abcam), mouse anti-active-β-catenin (clone 8E7; Millipore), rabbit anti-Syndecan4 (Abcam), rabbit anti-phospho-MLC2 (Thrl8/Ser19; Invitrogen), rabbit anti-phospho-FAK (Tyr397; Invitrogen), rabbit anti-phospho-S6 (S235/236; Cell Signaling Technology), rabbit anti-YAP (Cell Signaling Technology), mouse anti-embryonic myosin (DSHB), rabbit anti-DDX6 (Bethyl Laboratories Inc.) and DAPI (Life Technologies). Primary antibodies were visualized with fluorochrome conjugated secondary antibodies (Invitrogen). The stained fibers were mounted in Fluoromount-G mounting medium (SouthernBiotech). For most of the staining, the images were taken using a 20x Plan Fluor objective. Anti-Phospho-MLC2 and active Rho stained images were obtained with a 40x Plan Fluor objective and DDX6 stained images with a 60x Plan Fluor objective of the Nikon Eclipse Ti microscope. The filter settings, gain and exposure values were kept constant between experiments. The intensity of expression was determined by manually drawing a region of Interest (ROI) on a Pax7 positive SC. This will give the mean pixel intensity of the ROI in all the channels. The ROI is copied onto another region where there is no Pax7 positive cell to calculate the background intensity. The background intensity is subtracted and the mean intensity is plotted with GraphPad Prism 7. Representative images for antibody staining were taken using Leica DMi8 Confocal Microscope.

Circularity index measurement of SCs—Single muscle fibers were stained with anti-Syndecan4 and anti-Pax7 antibodies. The images were taken using a 20x Plan Fluor objective of Nikon Eclipse Ti microscope. Using the NIS Elements software and thresholding feature, a mask is drawn around the Pax7 positive cell. Care is taken to make sure that the mask overlaps the Syndecan4 (membrane) staining to include the membrane of the cell. The area and circularity index of the cell are measured by the software. The circularity index is a feature of how circular the cell is. It ranges from 0 to 1, with 1 being a perfect circle.

Quantitative PCR (qPCR)—Total RNA was isolated from single muscle fibers (from EDL muscle), or SCs using Trizol (Invitrogen) according to the manufacturer's protocol. The RNA was DNAse treated using Turbo DNA free kit (Life Technologies). cDNA was synthesized from RNA using the Superscript First Strand Synthesis System (Invitrogen). qPCR was performed in triplicates from 5ng of RNA per reaction using Platinum SYBR Green qPCR Super Mix-UDG w/ROX (Invitrogen) on a ViiA7 qPCR detection system (Life Technologies). All reactions for RT-qPCR were performed using the following conditions:

50°C for 2 min, 95°C for 2 min, 40 cycles of a two-step reaction of denaturation at 95°C for 15 min and annealing at 60°C for 30s. The mean Ct values from triplicates were used in the comparative $2^{-\Delta\Delta Ct}$ method. To analyze the expression of Wnt ligands on the adult muscle fiber, $2^{-\Delta Ct}$ method was used. The results were normalized to GAPDH mRNA controls. All primers used in this study are listed in Table S2.

Microarray—RNA was isolated from single muscle fibers of the EDL muscle from adult mouse hindlimb using TRIzol reagent (Invitrogen). The quality of the RNA was assessed with Agilent 2100 bioanalyzer. Processing of the RNA and hybridization to the Affymetrix GeneChip Mouse Gene 1.0 ST Arrays were performed by the Gladstone Institute Genomics Core. The array data sets were analyzed using GenePattern, a genomic analysis platform at the Broad Institute. The expression profiles were generated with annotated probes, background corrected and normalized using an RMA algorithm, resulting in a matrix containing one intensity value per probe set. All the expression values were log2 transformed and listed in Table S1

QUANTIFICATION AND STATISTICAL ANALYSIS

The statistical details of experiments can be found in the figure legends. No statistical methods were used to predetermine sample size. The investigators were not blinded to allocation during experiments and outcome assessment. No animal was excluded from analysis. All data are represented as mean +/− standard error of the mean (s.e.m). Significance was calculated using the two-tailed unpaired Student's t-tests (Graphpad Prism 7). The number of replicates (n) for each experiment is indicated in the figure legends. Differences were considered statistically different at $P<0.05$.

DATA AND CODE AVAILABILITY

The microarray data generated during this study are available at NCBI GEO-Accession Number GSE135163

Supplementary Material

Refer to Web version on PubMed Central for supplementary material.

ACKNOWLEDGEMENTS.

We would like to thank Drs. Karyn Esser, Richard R. Behringer, Ramesh A. Shivdasani, Charles Keller, Cord Brakebusch and Eric Olson for providing the mice. We would like to thank the members of the Brack laboratory for critical discussions in the preparation of this manuscript. We acknowledge the Parnassus Flow Cytometry Core at UCSF, supported in part by Grant NIH P30 DK063720 and NIH S10 1S10OD021822–01 and Chui K for technical assistance. This work was supported by NIH grants (R01AR060868, R01AR061002, R01AR076252) to ASB, NIH (F32AR067594) to SE and CIRM grant (RB5–07 409) and UCSF Discovery Fellowship to JMM.

REFERENCES.

Baghdadi MB, Firmino J, Soni K, Evano B, Di Girolamo D, Mourikis P, Castel D, and Tajbakhsh S (2018). Notch-Induced miR-708 Antagonizes Satellite Cell Migration and Maintains Quiescence. Cell Stem Cell 23, 859–+. [PubMed: 30416072]

Behrndt M, Salbreux G, Campinho P, Hauschild R, Oswald F, Roensch J, Grill SW, and Heisenberg CP (2012). Forces driving epithelial spreading in zebrafish gastrulation. Science 338, 257–260. [PubMed: 23066079]

Bischoff R (1990). Interaction between satellite cells and skeletal muscle fibers. Development 109, 943–952. [PubMed: 2226207]

Bjornson CRR, Cheung TH, Liu L, Tripathi PV, Steeper KM, and Rando TA (2012). Notch Signaling Is Necessary to Maintain Quiescence in Adult Muscle Stem Cells. Stem Cells 30, 232–242. [PubMed: 22045613]

Boonsanay V, Zhang T, Georgieva A, Kostin S, Qi H, Yuan X, Zhou Y, and Braun T (2016). Regulation of Skeletal Muscle Stem Cell Quiescence by Suv4–20h1-Dependent Facultative Heterochromatin Formation. Cell stem cell 18, 229–242. [PubMed: 26669898]

Brack AS, Conboy IM, Conboy MJ, Shen J, and Rando TA (2008). A temporal switch from Notch to Wnt signaling in muscle stem cells is necessary for normal adult myogenesis. Cell Stem Cell 2, 50–59. [PubMed: 18371421]

Brack AS, and Munoz-Canoves P (2016). The ins and outs of muscle stem cell aging. Skelet Muscle 6, 1. [PubMed: 26783424]

Brack AS, Murphy-Seiler F, Hanifi J, Deka J, Eyckerman S, Keller C, Aguet M, and Rando TA (2009). BCL9 is an essential component of canonical Wnt signaling that mediates the differentiation of myogenic progenitors during muscle regeneration. DevBiol.

Brack AS, and Rando TA (2007). Intrinsic changes and extrinsic influences of myogenic stem cell function during aging. Stem Cell Rev 3, 226–237. [PubMed: 17917136]

Burridge K, and Guilluy C (2016). Focal adhesions, stress fibers and mechanical tension. Exp Cell Res 343, 14–20. [PubMed: 26519907]

Chakkalakal JV, Christensen J, Xiang W, Tierney MT, Boscolo FS, Sacco A, and Brack AS (2014). Early forming label-retaining muscle stem cells require p27kip1 for maintenance of the primitive state. Development (Cambridge, England) 141,1649–1659.

Cheung TH, Quach NL, Charville GW, Liu L, Park L, Edalati A, Yoo B, Hoang P, and Rando TA (2012). Maintenance of muscle stem-cell quiescence by microRNA-489. Nature 482, 524–528. [PubMed: 22358842]

Cheung TH, and Rando TA (2013). Molecular regulation of stem cell quiescence. Nature reviews Molecular cell biology 14, 329–340. [PubMed: 23698583]

Chrzanowska-Wodnicka M, and Burridge K (1996). Rho-stimulated contractility drives the formation of stress fibers and focal adhesions. J Cell Biol 133,1403–1415. [PubMed: 8682874]

Clevers H, Loh KM, and Nusse R (2014). Stem cell signaling. An integral program for tissue renewal and regeneration: Wnt signaling and stem cell control. Science 346,1248012. [PubMed: 25278615]

Crist CG, Montarras D, and Buckingham M (2012). Muscle satellite cells are primed for myogenesis but maintain quiescence with sequestration of Myf5 mRNA targeted by microRNA-31 in mRNP granules. Cell Stem Cell 11,118–126. [PubMed: 22770245]

Dupont S (2016). Role of YAP/TAZ in cell-matrix adhesion-mediated signalling and mechanotransduction. Exp Cell Res 343, 42–53. [PubMed: 26524510]

Dupont S, Morsut L, Aragona M, Enzo E, Giulitti S, Cordenonsi M, Zanconato F, Le Digabel J, Forcato M, Bicciato S, et al. (2011). Role of YAP/TAZ in mechanotransduction. Nature 474, 179–183. [PubMed: 21654799]

Engler AJ, Sen S, Sweeney HL, and Discher DE (2006). Matrix elasticity directs stem cell lineage specification. Cell 126, 677–689. [PubMed: 16923388]

Figeac N, and Zammit PS (2015). Coordinated action of Axin1 and Axin2 suppresses beta-catenin to regulate muscle stem cell function. Cell Signal 27, 1652–1665. [PubMed: 25866367]

Gilbert PM, Havenstrite KL, Magnusson KE, Sacco A, Leonardi NA, Kraft P, Nguyen NK, Thrun S, Lutolf MP, and Blau HM (2010). Substrate elasticity regulates skeletal muscle stem cell self-renewal in culture. Science 329, 1078–1081. [PubMed: 20647425]

Goel AJ, Rieder MK, Arnold HH, Radice GL, and Krauss RS (2017). Niche Cadherins Control the Quiescence-to-Activation Transition in Muscle Stem Cells. Cell Rep 21, 2236–2250. [PubMed: 29166613]

Habas R, Dawid IB, and He X (2003). Coactivation of Rac and Rho by Wnt/Frizzled signaling is required for vertebrate gastrulation. Gene Dev 17, 295–309. [PubMed: 12533515]

Hyatt JP, Roy RR, Baldwin KM, and Edgerton VR (2003). Nerve activity-independent regulation of skeletal muscle atrophy: role of MyoD and myogenin in satellite cells and myonuclei. Am J Physiol Cell Physiol 285, C1161–1173. [PubMed: 12839833]

Jackson B, Peyrollier K, Pedersen E, Basse A, Karlsson R, Wang ZP, Lefever T, Ochsenbein AM, Schmidt G, Aktories K, et al. (2011). RhoA is dispensable for skin development, but crucial for contraction and directed migration of keratinocytes. Mol Biol Cell 22, 593–605. [PubMed: 21209320]

Jones AE, Price FD, Le Grand F, Soleimani VD, Dick SA, Megeney LA., and Rudnicki MA (2015). Wnt/beta-catenin controls follistatin signalling to regulate satellite cell myogenic potential. Skeletal muscle 5, 14. [PubMed: 25949788]

Judson RN, Tremblay AM, Knopp P, White RB, Urcia R, De Bari C, Zammit PS, Camargo FD, and Wackerhage H (2012). The Hippo pathway member Yap plays a key role in influencing fate decisions in muscle satellite cells. J Cell Sci 125, 6009–6019. [PubMed: 23038772]

Jussila M, and Ciruna B (2017). Zebrafish models of non-canonical Wnt/planar cell polarity signalling: fishing for valuable insight into vertebrate polarized cell behavior. Wires Dev Biol 6.

Kadowaki T, Wilder E, Klingensmith J, Zachary K, and Perrimon N (1996). The segment polarity gene porcupine encodes a putative multitransmembrane protein involved in Wingless processing. Genes Dev 10, 3116–3128. [PubMed: 8985181]

Kimmel JC, Chang AY, Brack AS, and Marshall WF (2018). Inferring cell state by quantitative motility analysis reveals a dynamic state system and broken detailed balance. PLoS Comput Biol 14, e1005927. [PubMed: 29338005]

Kimura K, Ito M, Amano M, Chihara K, Fukata Y, Nakafuku M, Yamamori B, Feng J, Nakano T, Okawa K, et al. (1996). Regulation of myosin phosphatase by Rho and Rho-associated kinase (Rho-kinase). Science 273, 245–248. [PubMed: 8662509]

Kobayashi A, Stewart CA, Wang Y, Fujioka K, Thomas NC, Jamin SP, and Behringer RR (2011). beta-Catenin is essential for Mullerian duct regression during male sexual differentiation. Development 138, 1967–1975. [PubMed: 21490063]

Komiya Y, and Habas R (2008). Wnt signal transduction pathways. Organogenesis 4, 68–75. [PubMed: 19279717]

Lacour F, Vezin E, Bentzinger CF, Sincennes MC, Giordani L, Ferry A, Mitchell R, Patel K, Rudnicki MA, Chaboissier MC, et al. (2017a). R-spondinl Controls Muscle Cell Fusion through Dual Regulation of Antagonistic Wnt Signaling Pathways. Cell Rep 18, 2320–2330. [PubMed: 28273449]

Lacour F, Vezin E, Bentzinger CF, Sincennes MC, Giordani L, Ferry A, Mitchell R, Patel K, Rudnicki MA, Chaboissier MC, et al. (2017b). R-spondin1 Controls Muscle Cell Fusion through Dual Regulation of Antagonistic Wnt Signaling Pathways. Cell reports 18, 2320–2330. [PubMed: 28273449]

Le Grand F, Jones AE, Seale V, Scime A, and Rudnicki MA (2009). Wnt7a Activates the Planar Cell Polarity Pathway to Drive the Symmetric Expansion of Satellite Stem Cells. Cell Stem Cell 4, 535–547. [PubMed: 19497282]

Lee HH, and Behringer RR (2007). Conditional Expression of Wnt4 during Chondrogenesis Leads to Dwarfism in Mice. Plos One 2.

Li L, and Fan CM (2017). A CREB-MPP7-AMOT Regulatory Axis Controls Muscle Stem Cell Expansion and Self-Renewal Competence. Cell Rep 21, 1253–1266. [PubMed: 29091764]

Machado L, Esteves de Lima J, Fabre O, Proux C, Legendre R, Szegedi A, Varet H, Ingerslev LR, Barres R, Relaix F, et al. (2017). In Situ Fixation Redefines Quiescence and Early Activation of Skeletal Muscle Stem Cells. Cell Rep 21, 1982–1993. [PubMed: 29141227]

McCarthy JJ, Srikuea R, Kirby TJ, Peterson CA, and Esser KA (2012). Inducible Cre transgenic mouse strain for skeletal muscle-specific gene targeting. Skelet Muscle 2, 8. [PubMed: 22564549]

Mikels AJ, and Nusse R (2006). Purified Wnt5a protein activates or inhibits beta-catenin-TCF signaling depending on receptor context. PLoS Biol 4, e115. [PubMed: 16602827]

Morel BG, Chretien F, and Tajbakhsh S (2009). Skeletal muscle as a paradigm for regenerative biology and medicine. Regen Med 4, 293–319. [PubMed: 19317647]

Mourikis P, Sambasivan R, Castel D, Rocheteau P, Bizzarro V, and Tajbakhsh S (2011). A Critical Requirement for Notch Signaling in Maintenance of the Quiescent Skeletal Muscle Stem Cell State. Stem cells (Dayton, Ohio).

Mourikis P, Sambasivan R, Castel D, Rocheteau P, Bizzarro V, and Tajbakhsh S (2012). A critical requirement for notch signaling in maintenance of the quiescent skeletal muscle stem cell state. Stem Cells 30, 243–252. [PubMed: 22069237]

Murphy MM, Keefe AC, Lawson JA, Flygare SD, Yandell M, and Kardon G (2014). Transiently Active Wnt/beta-Catenin Signaling Is Not Required but Must Be Silenced for Stem Cell Function during Muscle Regeneration. Stem Cell Rep 3, 475–488.

Nabhan AN, Brownfield DG, Harbury PB, Krasnow MA, and Desai TJ (2018). Single-cell Wnt signaling niches maintain sternness of alveolar type 2 cells. Science 359, 1118–+. [PubMed: 29420258]

Nishijo K, Hosoyama T, Bjornson CR, Schaffer BS, Prajapati SI, Bahadur AN, Hansen MS, Blandford MC, McCleish AT., Rubin BP, et al. (2009). Biomarker system for studying muscle, stem cells, and cancer in vivo. FASEB J 23, 2681–2690. [PubMed: 19332644]

Orford KW, and Scadden DT (2008). Deconstructing stem cell self-renewal: genetic insights into cell-cycle regulation. NatRevGenet 9, 115–128.

Parisi A, Lacour F, Giordani L, Colnot S, Maire P, and Le Grand F (2015a). APC is required for muscle stem cell proliferation and skeletal muscle tissue repair. J Cell Biol 210, 717–726. [PubMed: 26304725]

Parisi A, Lacour F, Giordani L, Colnot S, Maire P, and Le Grand F (2015b). APC is required for muscle stem cell proliferation and skeletal muscle tissue repair. The Journal of cell biology 210, 717–726. [PubMed: 26304725]

Polesskaya A, Seale P, and Rudnicki MA (2003). Wnt signaling induces the myogenic specification of resident CD45+ adult stem cells during muscle regeneration. Cell 113, 841–852. [PubMed: 12837243]

Proffitt KD, and Virshup DM (2012). Precise Regulation of Porcupine Activity Is Required for Physiological Wnt Signaling. J Biol Chem 287, 34167–34178. [PubMed: 22888000]

Ridley AJ, and Hall A (1992). The small GTP-binding protein rho regulates the assembly of focal adhesions and actin stress fibers in response to growth factors. Cell 70, 389–399. [PubMed: 1643657]

Rodgers JT, King KY, Brett JO, Cromie MJ, Charville GW, Maguire KK, Brunson C, Mastey N, Liu L, Tsai CR, et al. (2014). mTORC1 controls the adaptive transition of quiescent stem cells from G0 to G(Alert). Nature 510, 393–396. [PubMed: 24870234]

Rodgers JT, Schroeder MD, Ma C, and Rando TA (2017). HGFA Is an Injury-Regulated Systemic Factor that Induces the Transition of Stem Cells into GAIert. Cell Rep 19, 479–486. [PubMed: 28423312]

Roman AKS, Jayewickreme CD, Murtaugh LC, and Shivdasani RA (2014). Wnt Secretion from Epithelial Cells and Subepithelial Myofibroblasts Is Not Required in the Mouse Intestinal Stem Cell Niche In Vivo. Stem Cell Rep 2, 127–134.

Rudolf A, Schirwis E, Giordani L, Parisi A, Lepper C, Taketo MM, and Le Grand F (2016). beta-Catenin Activation in Muscle Progenitor Cells Regulates Tissue Repair. Cell reports 15, 1277–1290. [PubMed: 27134174]

Schlessinger K, Hall A, and Tolwinski N (2009). Wnt signaling pathways meet Rho GTPases. Gene Dev 23, 265–277. [PubMed: 19204114]

Schreck C, Istvanffy R, Ziegenhain C, Sippenauer T, Ruf F, Henkel L, Gartner F, Vieth B, Florian MC, Mende N, et al. (2017). Niche WNT5A regulates the actin cytoskeleton during regeneration of hematopoietic stem cells. J Exp Med 214,165–181. [PubMed: 27998927]

Seo J, and Kim J (2018). Regulation of Hippo signaling by actin remodeling. Bmb Rep 51,151–156. [PubMed: 29353600]

Sit ST, and Manser E (2011). Rho GTPases and their role in organizing the actin cytoskeleton. J Cell Sci 124, 679–683. [PubMed: 21321325]

Sokol SY (2015). Spatial and temporal aspects of Wnt signaling and planar cell polarity during vertebrate embryonic development. Semin Cell Dev Biol 42, 78–85. [PubMed: 25986055]

Strochlic L, Falk J, Goillot E, Sigoillot S, Bourgeois F, Delers P, Rouviere J, Swain A, Castellani V, Schaeffer L, et al. (2012). Wnt4 participates in the formation of vertebrate neuromuscular junction. Plos One 7, e29976. [PubMed: 22253844]

Sun C, De Mello V, Mohamed A, Ortuste Quiroga HP, Garcia-Munoz A, Al Bloshi A, Tremblay AM, von Kriegsheim A, Collie-Duguid E, Vargesson N, et al. (2017). Common and Distinctive Functions of the Hippo Effectors Taz and Yap in Skeletal Muscle Stem Cell Function. Stem Cells 35, 1958–1972. [PubMed: 28589555]

Tammela T, Sanchez-Rivera FJ, Cetinbas NM, Wu K, Joshi NS, Helenius K, Park Y, Azimi R, Kerper NR, Wesselhoeft RAL, et al. (2017). A Wnt-producing niche drives proliferative potential and progression in lung adenocarcinoma. Nature 545, 355–+. [PubMed: 28489818]

Topol L, Jiang X, Choi H, Garrett-Beal L, Carolan PJ, and Yang Y (2003). Wnt-5a inhibits the canonical Wnt pathway by promoting GSK-3-independent beta-catenin degradation. J Cell Biol 162, 899–908. [PubMed: 12952940]

Tremblay AM, Missiaglia E, Galli GG, Hettmer S, Urcia R, Carrara M, Judson RN, Thway K, Nadal G, Selfe JL, et al. (2014). The Hippo transducer YAP1 transforms activated satellite cells and is a potent effector of embryonal rhabdomyosarcoma formation. Cancer Cell 26, 273–287. [PubMed: 25087979]

van den Brink SC, Sage F, Vertesy A, Spanjaard B, Peterson-Maduro J, Baron CS, Robin C, and van Oudenaarden A (2017). Single-cell sequencing reveals dissociation-induced gene expression in tissue subpopulations. Nat Methods 14, 935–936. [PubMed: 28960196]

van Velthoven CTJ, de Morree A, Egner IM, Brett JO, and Rando TA (2017). Transcriptional Profiling of Quiescent Muscle Stem Cells In Vivo. Cell Rep 21, 1994–2004. [PubMed: 29141228]

von Maltzahn J, Bentzinger CF, and Rudnicki MA (2012). Wnt7a-Fzd7 signalling directly activates the Akt/mTOR anabolic growth pathway in skeletal muscle. Nat Cell Biol 14, 186–191.

Westfall TA, Brimeyer R, Twedt J, Gladon J, Olberding A, Furutani-Seiki M, and Slusarski DC (2003). Wnt-5/pipetail functions in vertebrate axis formation as a negative regulator of Wnt/beta-catenin activity. J Cell Biol 162, 889–898. [PubMed: 12952939]

Windisch A, Gundersen K, Szabolcs MJ, Gruber H, and Lomo T (1998). Fast to slow transformation of denervated and electrically stimulated rat muscle. The Journal of physiology 510 (Pt 2), 623–632. [PubMed: 9706009]

Xin M, Kim Y, Sutherland LB, Qi X, McAnally J, Schwartz RJ, Richardson JA, Bassel-Duby R, and Olson EN (2011). Regulation of insulin-like growth factor signaling by Yap governs cardiomyocyte proliferation and embryonic heart size. Sci Signal 4, ra70. [PubMed: 22028467]

Yang YZ, and Mlodzik M (2015). Wnt-Frizzled/Planar Cell Polarity Signaling: Cellular Orientation by Facing the Wind (Wnt). Annu Rev Cell Dev Bi 31, 623–646.

Zepp JA, Zacharias WJ, Frank DB, Cavanaugh CA, Zhou S, Morley MP, and Morrisey EE (2017). Distinct Mesenchymal Lineages and Niches Promote Epithelial Self-Renewal and Myofibrogenesis in the Lung. Cell 170, 1134–1148. [PubMed: 28886382]

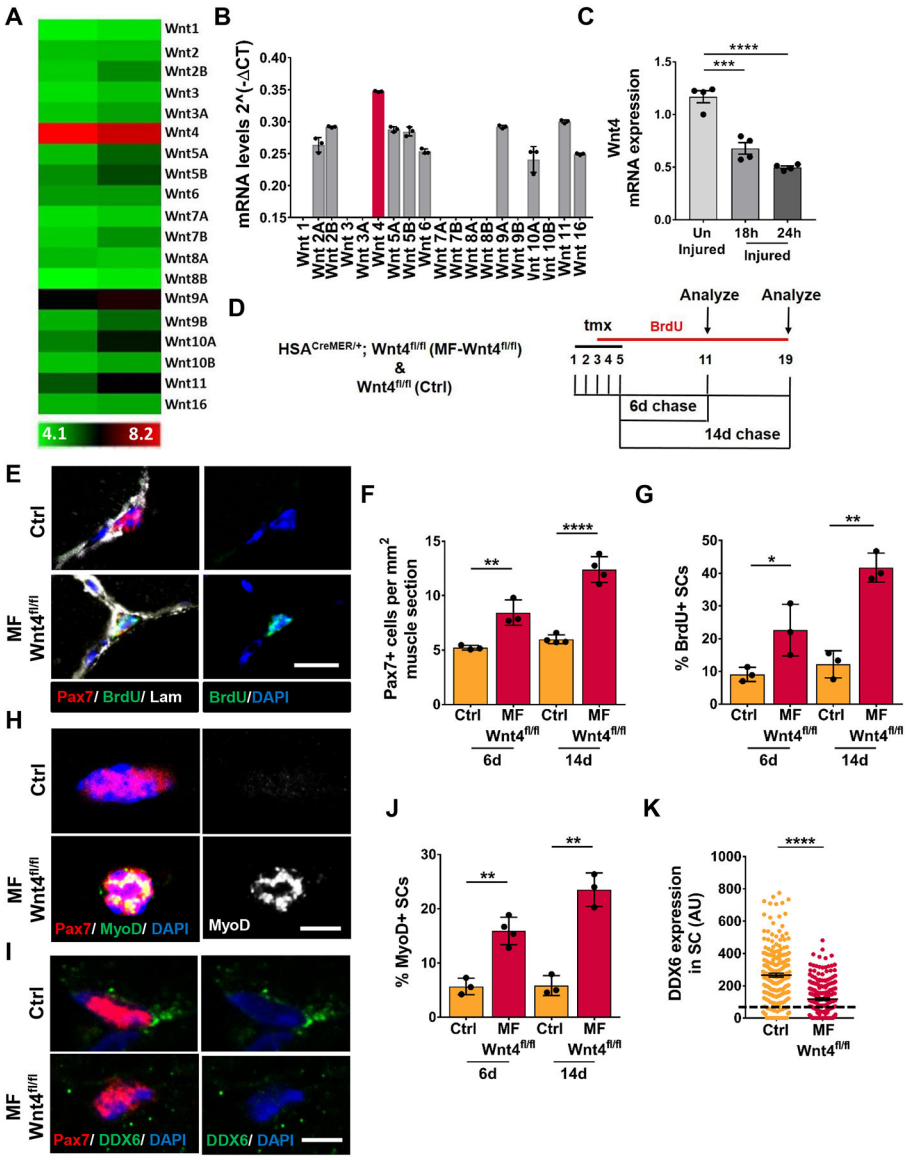

Figure 1. Wnt4 from the adult muscle fiber maintains SC quiescence.

(A) Heatmap of the gene expression levels of Wnt ligands from microarray of isolated adult single muscle fibers (n=2). The expression values are log2 transformed and range from 4.1 (low-green) to 8.2 (high-red).

(B) qRT-PCR of Wnt ligands in isolated wildtype adult single muscle fibers from the EDL. The individual Wnts were normalized to GAPDH (n=3).

(C) Wnt4 mRNA expression by qRT-PCR from wildtype uninjured, 18h and 24h injured TA muscle.

(D) Schematic representation of the experimental design.

(E-F) Representative images (E) and quantification (F) of $Pax7^{+}$ cells per $1mm^2$ TA section of Control and Myofiber-$Wnt4^{fl/fl}$, 6d and 14d post tmx (n=>3).

(G) Quantification of $BrdU^{+}$ SCs in Control and Myofiber-$Wnt4^{fl/fl}$ TA sections, 6d and 14d post tmx (n=3).

(H and J) Representative images (H) and quantification (J) of $MyoD^{+}$ SCs in control and Myofiber-$Wnt4^{fl/fl}$ single muscle fibers, 6d and 14d post tmx (n=>3).
(I and K) Representative images (I) and quantification (K) of DDX6 intensity in SCs in control and Myofiber-$Wnt4^{fl/fl}$ TA muscle sections, 6d and 14d post tmx (n=3). The dashed line represents the threshold of intensity visible by eye.
Error bars, s.e.m.; *P<0.05, **P<0.01, ***P<0.001, ****P<0.0001; Scale bars 10μm in (E), 5μm in (H and I).

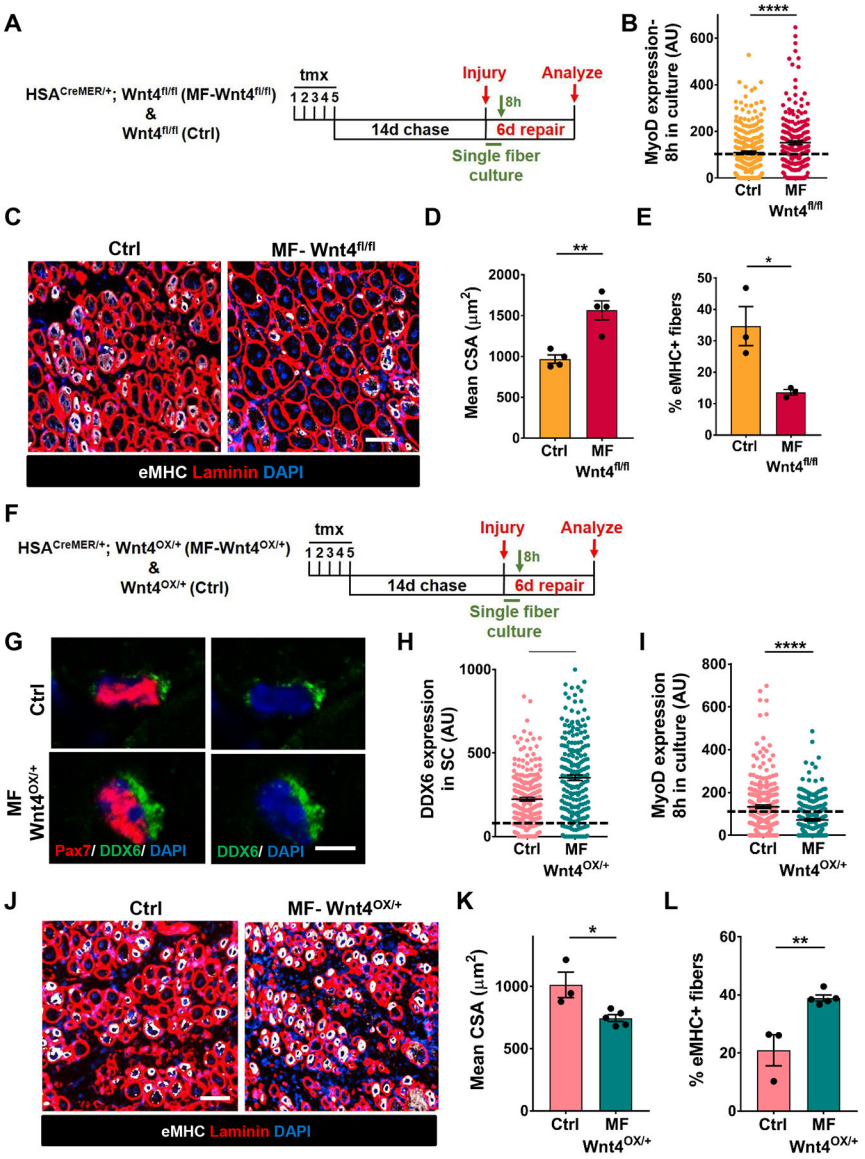

Figure 2. Wnt4 from the niche regulates muscle regeneration.

(A) Schematic representation of the experimental design.

(B) Quantification of MyoD expression in SCs on Control and Myofiber-Wnt4$^{fll/fl}$ muscle fibers, cultured *in vitro* for 8h (n=3).

(C and D) Representative images (C) and quantification (D) of the cross-sectional area of centrally nucleated fibers in Control and Myofiber-Wnt4$^{fl/fl}$ TAs injured and regenerated for 6d (n=4).

(E) Percentage of fibers that express Embryonic Myosin Heavy Chain in Control and Myofiber-Wnt4$^{fl/fl}$ TA sections after 6d of regeneration (n=3).

(F) Schematic representation of the experimental design.

(G and H) Representative images (G) and quantification (H) of DDX6 intensity of SCs in Control and Myofiber-Wnt4$^{OX/+}$ TA muscle sections, 14d after tmx (n=3).

(I) Quantification of MyoD expression in SCs on Control and Myofiber-Wnt4$^{OX/+}$ muscle fibers, cultured *in vitro* for 8h (n=3).
(J and K) Representative images (J) and quantification (K) of the cross-sectional area of centrally nucleated fibers in control and Myofiber-Wnt4$^{OX/+}$ TAs injured and regenerated for 6d (n=4).
(L) Percentage of fibers that express Embryonic Myosin Heavy Chain in Control and Myofiber-Wnt4$^{OX/+}$ TA muscle sections after 6d of regeneration (n=3).
The dashed line in Figures 2B, 2H and 2I represents the threshold of intensity visible by eye. Error bars, s.e.m.; *P<0.05, **P<0.01, ****P<0.0001; Scale bars 50μm in (C and J), 5μm in (G).

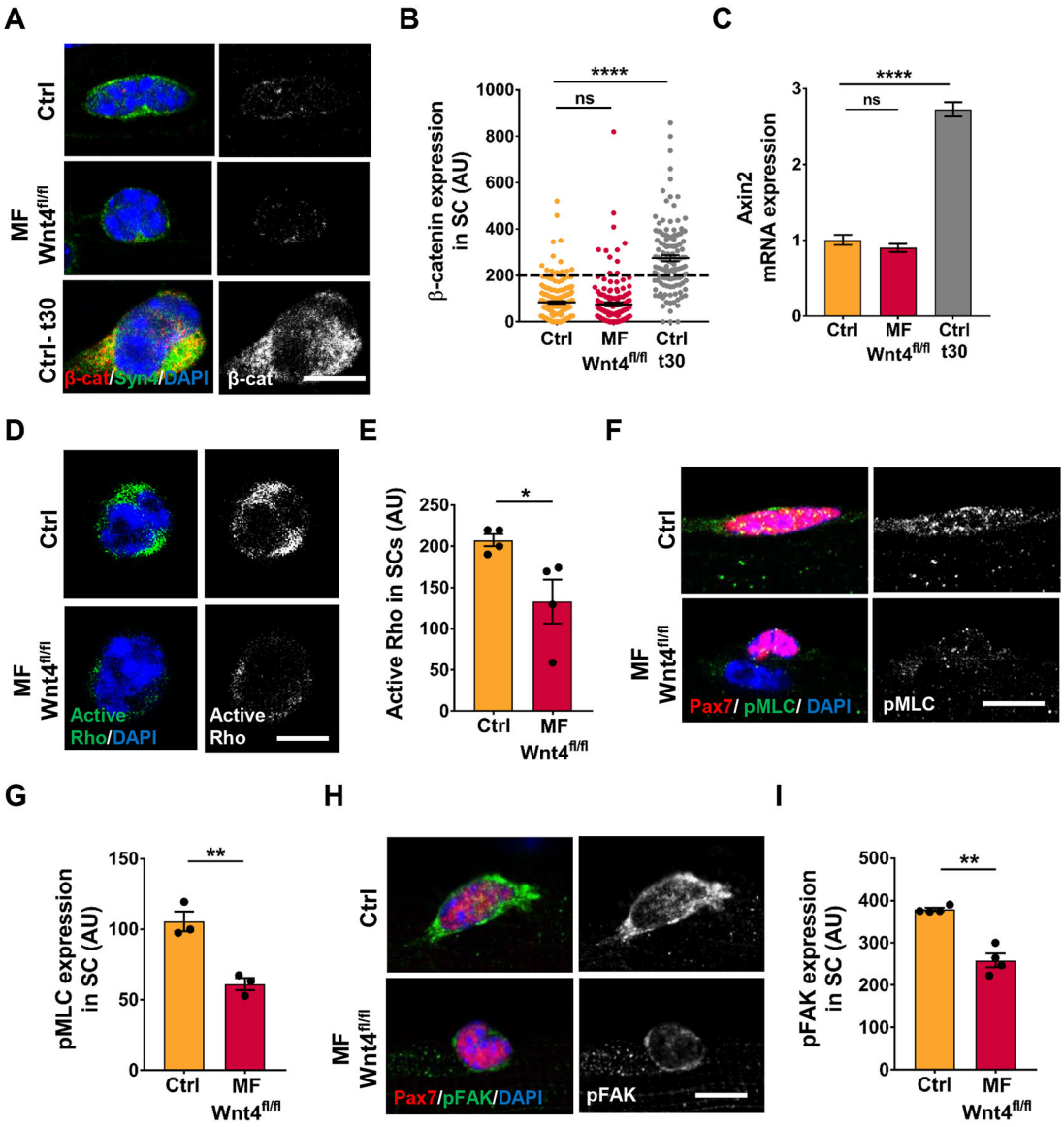

Figure 3. Niche-derived Wnt4 signals via Rho/cytoskeletal signaling.

(A and B) Representative images (A) and quantification (B) of active β-catenin expression in SCs on Control and Myofiber-Wnt4$^{fl/fl}$ isolated single muscle fibers, 14d post tmx and on WT fibers cultured *in vitro* for 30h (n=3). The dashed line represents the threshold of intensity visible by eye.

(C) Axin2 mRNA expression by qRT-PCR in FACS isolated Control and Myofiber-Wnt4$^{fl/fl}$ SCs, 14d post tmx and on WT SCs cultured *in vitro* for 30h (n=3).

(D and E) Representative images (D) and quantification (E) of active Rho levels in SCs from Control and Myofiber-Wnt4$^{fl/fl}$ single fibers 14d post tmx (n=4).

(F and G) Representative images (F) and quantification (G) of pMLC expression in SCs from Control and Myofiber-Wnt4$^{fl/fl}$ single fibers, 14d post tmx (n=3).

(H and I) Representative images (H) and quantification (I) of pFAK expression in SCs from Control and Myofiber-Wnt4$^{fl/fl}$ single fibers, 14d post tmx (n=4).

Error bars, s.e.m.; *P<0.05, **P<0.01, ****P<0.0001; Scale bars 5μm in (A, D, F and H).

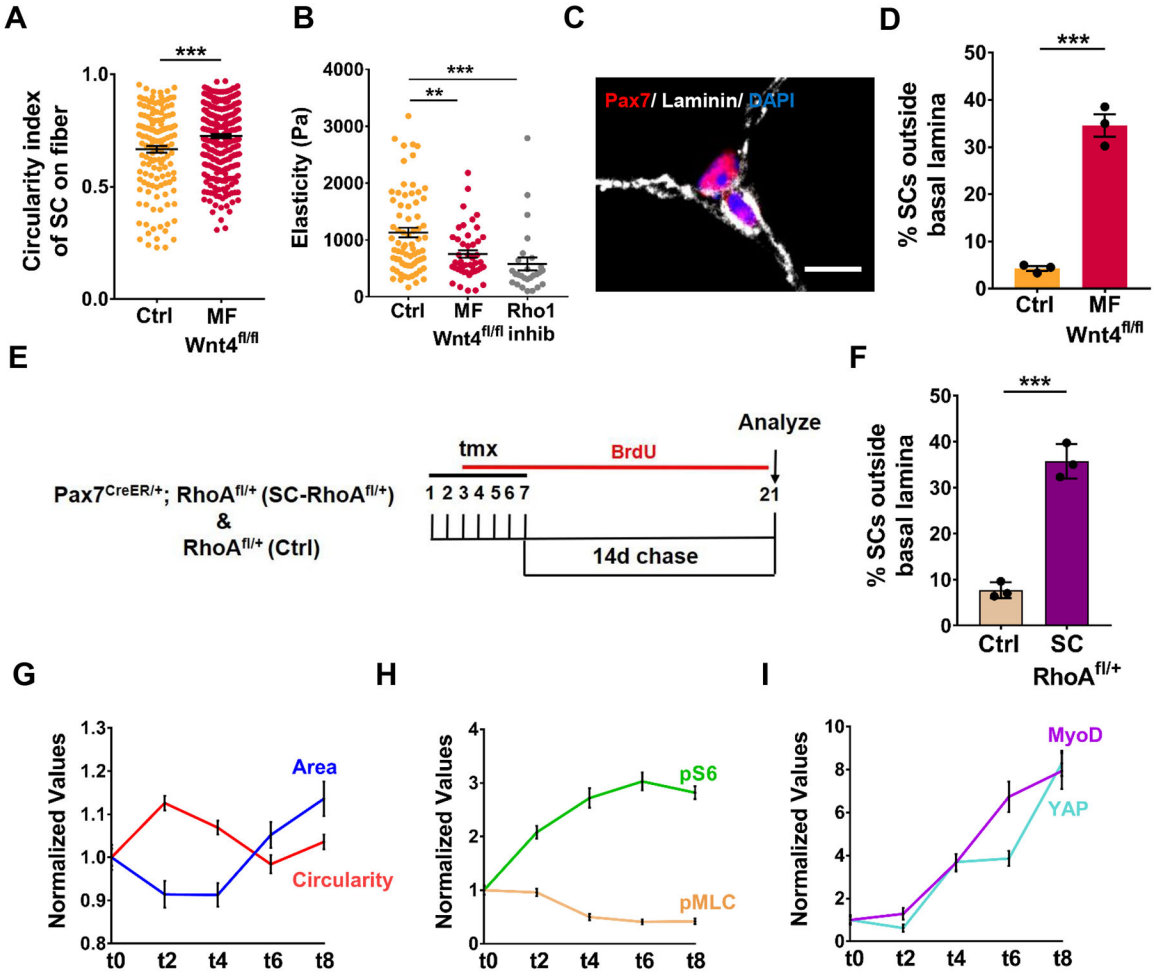

Figure 4. Wnt4-Rho signaling axis regulates mechano-properties and retains QSCs in the niche.

(A) Circularity index of SCs on Control and Myo fiber-Wnt4$^{fl/fl}$ isolated muscle fibers, 14d post tmx (n=3).

(B) The elasticity of QSCs as measured by AFM in Control and Myofiber-Wnt4$^{fl/fl}$ FACS isolated SCs fixed immediately, 14d post tmx and in SCs treated with Rho1 inhibitor *in vitro* for 2h (n=3).

(C and D) Representative images (C) and quantification (D) of SCs outside the basal lamina in Control and Myofiber-Wnt4$^{fl/fl}$ TA muscle sections, 14d post tmx (n=3).

(E) Schematic representation of the experimental design.

(F) Percentage of SCs outside the basal lamina in Control and SC-RhoA$^{fl/+}$TA muscle sections, 14d post tmx (n=3).

(G) Normalized values of Circularity and Area of WT SCs on isolated single muscle fibers, fixed immediately (t0) or cultured *in vitro* for different time points (n=3). The mean of t0 was kept at 1 and all the other time points were normalized to t0. The raw data is in Figure S4.

(H) Normalized values of pS6 and pMLC expression in WT SCs on isolated single muscle fibers, fixed immediately (t0) or cultured *in vitro* for different time points (n=3).

(I) Normalized values of MyoD and YAP expression in WT SCs on isolated single muscle fibers, fixed immediately (t0) or cultured *in vitro* for different time points (n=3).
Error bars, s.e.m.; **P<0.01, ***P<0.001; Scale bar 10μm in (C).

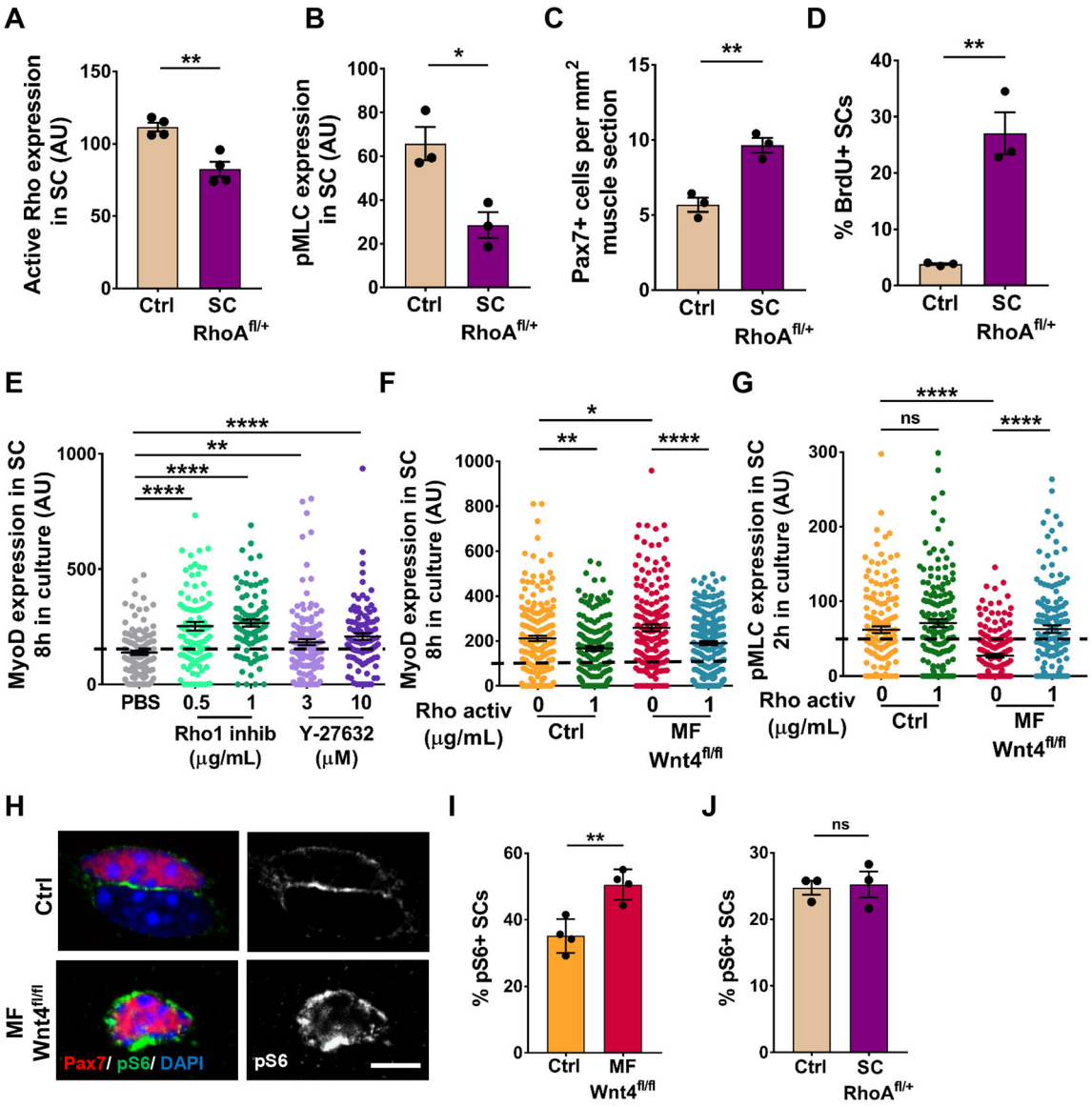

Figure 5. Niche derived Wnt4 signals via RhoA to promote quiescence.

(A) Quantification of active Rho expression in Control and SC-RhoA$^{fl/+}$FACS isolated SCs, 14d post tmx (n=3).

(B) Quantification of pMLC expression in SCs on Control and SC-RhoA$^{fl/+}$ isolated single muscle fibers, 14d post tmx (n=3).

(C) Quantification of Pax7^{+} cells per 1mm^{2} TA muscle section of Control and SC-RhoA$^{fl/+}$, 14d post tmx (n=3).

(D) Percentage of BrdU^{+} SCs in Control and SC-RhoA$^{fl/+}$ TA muscle sections, 14d post tmx (n=3).

(E) MyoD expression in SCs on isolated muscle fibers treated with PBS, Rhol inhibitor or ROCK inhibitor for 8h *in vitro* (n=2).

(F) MyoD expression in SCs on muscle fibers from Control and Myofiber-Wnt4$^{fl/fl}$ treated with Rho activator for 8h *in vitro* (n=3).

(G) pMLC expression in SCs on muscle fibers from Control and Myofiber-Wnt4$^{fl/fl}$ treated with Rho activator for 2h *in vitro* (n=3).
(H and I) Representative images (H) and quantification (I) of the percent pS6^{+} SCs on Control and Myofiber-Wnt4$^{fl/fl}$ muscle fibers, 14d post tmx (n=4).
(J) Percentage of pS6^{+} SCs on Control and SC-RhoA$^{fl/+}$ muscle fibers, 14d post tmx (n=3).
The dashed line in Figures 5E, 5F and 5G represents the threshold of intensity visible by eye.
Error bars, s.e.m.; *P<0.05, **P<0.01, ****P<0.0001; Scale bars 5μm in (H).

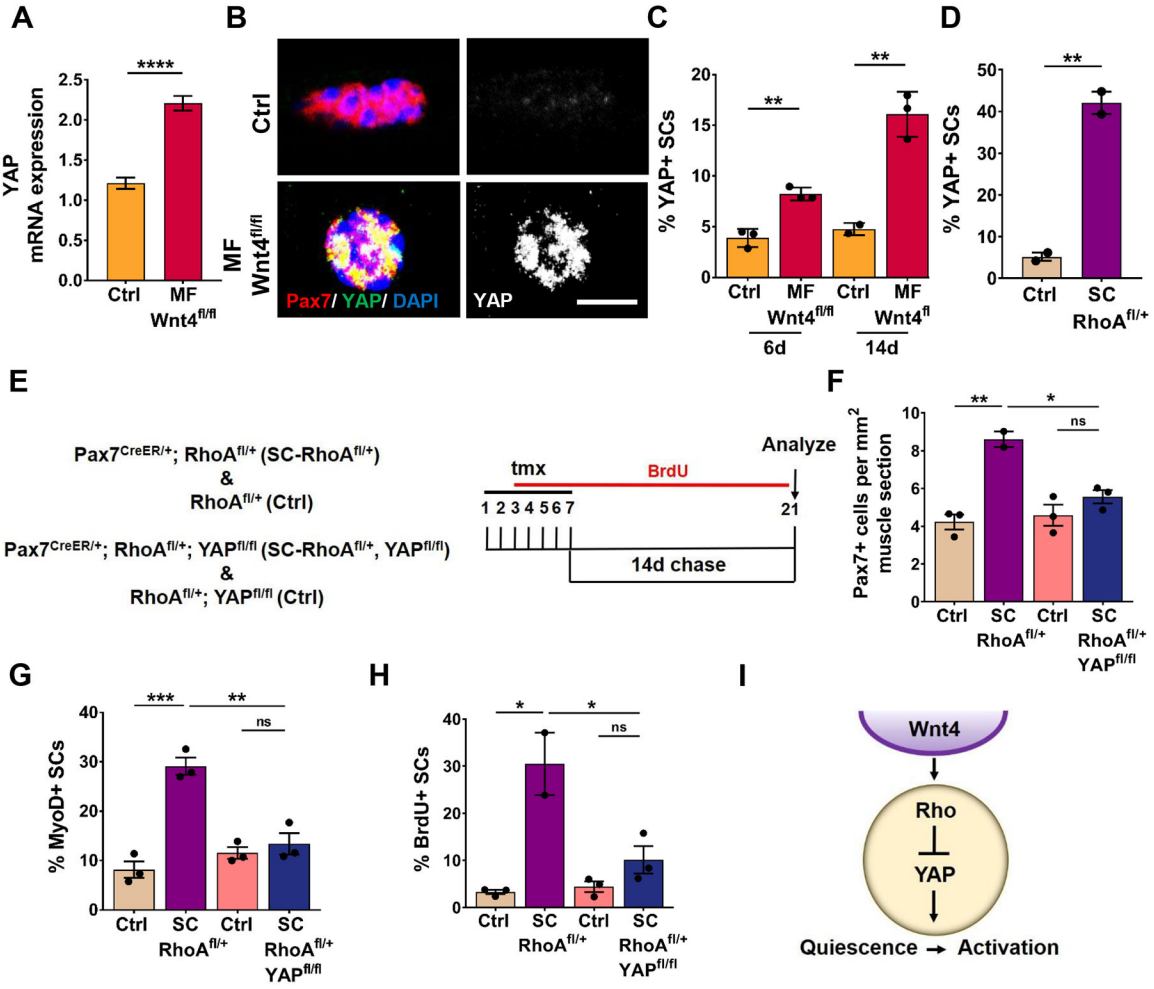

Figure 6. Wnt-Rho regulated activation is dependent on YAP.

(A) YAP mRNA expression by qRT-PCR in Control and Myofiber-Wnt4$^{fl/fl}$ FACs isolated SCs (n=5).

(B and C) Representative images (B) and quantification (C) of YAP positive SCs in Control and Niche-Wnt4$^{fl/fl}$ isolated muscle fibers, 6d and 14d post tmx (n=3).

(D) Percentage of YAP^{+} SCs on Control and SC-RhoA$^{fl/+}$ muscle fibers, 14d post tmx (n=3).

(E) Schematic representation of the experimental design.

(F) Quantification of Pax7^{+} cells per 1mm^{2} TA muscle section of Control, SC-RhoA$^{fl/+}$ and Control, SC-RhoA$^{fl/+}$, YAP$^{fl/fl}$, 14d post tmx (n=3).

(G) Quantification of the percentage of MyoD^{+} SCs in Control, SC-RhoA$^{fl/+}$ and Control, SC-RhoA$^{fl/+}$, YAP$^{fl/fl}$ isolated single muscle fibers, 14d post tmx (n=3).

(H) Quantification of the percentage of BrdU^{+} SCs in Control, SC-RhoA$^{fl/+}$ and Control, SC-RhoA$^{fl/+}$, YAP$^{fl/fl}$ TA muscle sections, 14d post tmx (n=3).

(I) Model depicting Wnt4 from the niche regulates Rho in the SC which represses YAP, thus preventing the SC quiescence to activation transition.

Error bars, s.e.m.; *P<0.05, **P<0.01, ***P<0.001, ****P<0.0001; Scale bars 5μm in (B).